ACS APPLIED MATERIALS & INTERFACES

www.acsami.org

Research Article

Label-Free Analysis of H5N1 Virus Based on Three-Segment Branched DNA-Templated Fluorescent Silver Nanoclusters

Ying Zhang, Fei Mu, Yefan Duan, Qi Li, Yating Pan, Hongfang Du, Panpan He, Xizhong Shen, Zhimin Luo,* Changfeng Zhu,* and Lianhui Wang*

Cite This: https://dx.doi.org/10.1021/acsami.0c14509

Read Online

ACCESS | Metrics & More | Article Recommendations | Supporting Information

ABSTRACT: Since H5N1 virus is a highly infectious pathogen that causes outbreaks of avian influenza, developing a sensitive and rapid diagnostic platform to sense it becomes significant. Here, a novel label-free fluorescence sensing platform based on DNA-templated silver nanoclusters (DNA-Ag NCs) is developed to detect the H5N1 gene sequence representing H5N1 virus. The three-segment-branched DNA structure with closed cytosine-rich loop is designed as an effective template to produce fluorescent Ag NCs, which is different with the previous design of cytosine-rich loop formed by hairpin-like single-stranded DNA or double-stranded DNA. The proposed fluorescence detection approach gives a wide linear range (500 pM-2 μM) and a low detection limit (500 pM) to sense H5N1 gene sequence. Furthermore, selective analysis of target DNA shows that our constructed analytical strategy has a high selectivity to H5N1 gene sequence. It is regarded as a promising method for highly sensitive and selective sensing of H5N1 virus.

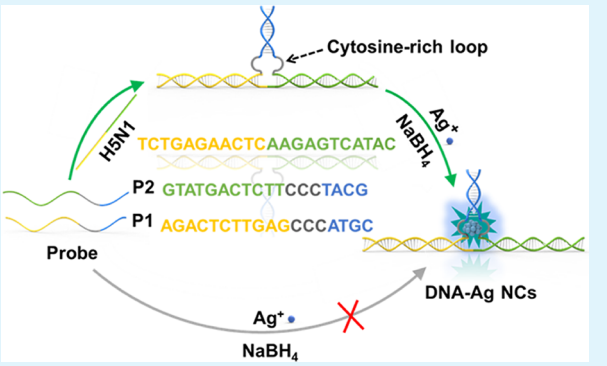

KEYWORDS: *fluorescent silver nanoclusters, DNA template manipulation, three-segment-branched DNA, H5N1 virus, biosensor*

INTRODUCTION

H5N1 avian influenza virus, a kind of highly contagious pathogen, has a high mortality rate and poses a serious threat to world health security.[1−3] Currently, sensitive and rapid diagnosis of H5N1 virus is extremely urgent for early diagnosis of avian influenza viruses. Although some methods have been used to detect H5N1 virus, such as serology differentiation,[4,5] surface plasma resonance (SPR),[6] enzyme-linked immune sorbent assay (ELISA),[7] reverse transcription-polymerase chain reaction (RT-PCR),[8,9] etc., they are often laborious, time-consuming, and have low sensitivity. Analytical methods based on a fluorescent molecular beacon have attracted great attention because of their simplicity, rapidness, and high sensitivity, but the poor photostability of traditional organic molecules restricts their applications.[10] It is desired to develop a more stable, efficient, and specific fluorescence sensing platform to sense H5N1 virus.

Fluorescence biosensors based on silver nanoclusters (Ag NCs) have become a powerful analytical tool due to their good optical stability, biocompatibility, and adjustable fluorescence characteristics.[11,12] DNA-templated Ag NCs (DNA-Ag NCs) integrating the programmable structure and specific recognition ability of nucleotides have been widely used for sensing nucleic acid markers,[13−15] proteins,[16,17] viruses,[18,19] and other small biomolecules.[20,21] The abundant DNA structures with smart editability can precisely regulate the crystal structures and fluorescence properties of noble-metal NCs.[22] Three-segment-branched DNA structures fabricated by assembling multiple DNA strands can provide a unique conformational flexibility to grow and stabilize DNA-Ag NCs at its multiple sites. For example, Park et al.[23] and Yang et al.[24] designed a Y-shaped three-segment-branched DNA structure to synthesize Ag NCs, which proved to be effective and robust in stabilizing Ag NCs. However, noble-metal NCs can only form on the outside of designed double-stranded DNA or at the end of designed DNA strands in these reported three-segment branched DNA structures, which restricts it when applied to specifically detect nucleic acid targets such as H5N1 gene sequences. Compared to fully matched linear double-stranded DNA, three-segment DNA structures with nucleotide mutation, mismatch, or terminal protrusion are more beneficial for the formation of noble-metal NCs.[25] Three-segment DNA structures containing base-mismatched DNA sequences and cytosine-rich loops can provide more active sites to form and stabilize noble-metal NCs,[26,27] which is expected to be an

Received: August 12, 2020
Accepted: October 2, 2020

effective template to prepare Ag NCs for the fabrication of fluorescence biosensors.

Here, a novel label-free fluorescence sensing platform based on three-segment-branched DNA-Ag NCs is developed to detect the H5N1 genomic fragment representing H5N1 virus, which is referred to as "H5N1" in our work. The three-segment-branched DNA structure containing mismatched and cytosine-rich nucleotide sequence is designed as a template to form fluorescent Ag NCs. The probe sequence can be modulated according to the nucleic acid sequence of targets. Our design concept can be extended to fabricate various nucleic acid probes for sensing different targets. The proposed fluorescent DNA-Ag NC-based method for sensing H5N1 is presented in Scheme 1. Two oligonucleotide strands are designated as probe 1 (P1) and probe 2 (P2) for detecting H5N1. The middle cytosine-rich segments (black line) of both P1 and P2 are the regions where Ag NCs are formed. Since only the front part (blue line) of P1 and P2 can pair with each other and the corresponding opposite end is designed to pair with half of the base sequence of H5N1, P1 and P2 cannot completely hybridize. After the addition of H5N1, complementary base pairing occurs among P1, P2, and H5N1 to form a three-segment-branched DNA structure with closed cytosine-rich loop, in which silver ions (Ag^+) are chelated. DNA-Ag NCs are produced by chemically reducing Ag^+ with $NaBH_4$. The qualitative and quantitative detection of H5N1 can be realized according to the fluorescence change of formed DNA-Ag NCs before and after adding H5N1.

Scheme 1. Formation of Fluorescent DNA-Ag NCs with Three-Segment-Branched DNA Structure as a Template to Detect H5N1

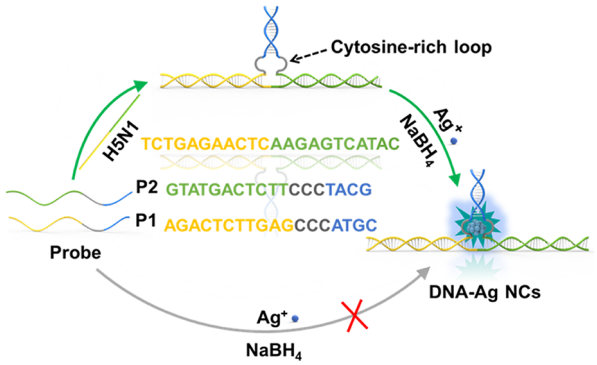

EXPERIMENTAL SECTION

Materials and Reagents. $NaBH_4$ (>99%) and $AgNO_3$ (>99%) were bought from Sigma-Aldrich. Fetal bovine serum (FBS) and DNA strands were provided by Sangon (Shanghai, China). Table S1 lists the sequences of used DNA. The citrate buffer solution (CBS) was purchased from Zhejiang Lianshuo Biotechnology Co., Ltd. (Zhejiang China). All the solutions were prepared with deionized water and stored at 4 °C in the experiments. In our experiments, a 22 base detection target was used to represent the H5N1 virus, since it is the representative sequence in the entire genome of H5N1 virus according to the gene library.

Characterizations. Transmission electron microscopy (TEM) images of DNA-Ag NCs were taken on an HT7700 (Hitachi, Japan) with an acceleration voltage of 100 kV. High-resolution TEM (HRTEM) characterization was performed on a JEM-2100F (JEOL, Japan) with an acceleration voltage of 200 kV. Ultraviolet−visible (UV−vis) absorption spectra and fluorescence spectra were recorded by a Shimadzu UV-3600 UV−vis spectrophotometer and Shimadzu RF-5301PC fluorophotometer, respectively.

Synthesis of DNA-Ag NCs. DNA-Ag NCs were synthesized using $NaBH_4$ as a reducing agent and three-segment-branched DNA structure as a growth template. Briefly, P1 (20 μL, 100 μM) and P2 (20 μL, 100 μM) were added in CBS (pH = 7.0, 20 mM), and then 20 μL of H5N1 (100 μM) was added to hybridize with P1 and P2. A total of 60 μL of $AgNO_3$ aqueous solution (400 μM) was added and shaken vigorously for 1 min. The mixed solution was then incubated for 30 min in the dark. After that, 60 μL of freshly prepared $NaBH_4$ solution (400 μM) was quickly added and shaken vigorously for 30 min. Finally, the whole solution was incubated for 24 h at 4 °C in the dark before fluorescence measurements. Different pH values (5.0, 6.0, 7.0, and 8.0) and temperatures (4, 20, and 37 °C) of reacted solutions were investigated to explore their influences on the formation of DNA-Ag NCs.

Qualitative and Quantitative Detection of H5N1. In the process of H5N1 detection, 2 μM of probes (P1 and P2) solution was prepared. A total of 20 μL of H5N1 with different concentrations (0−

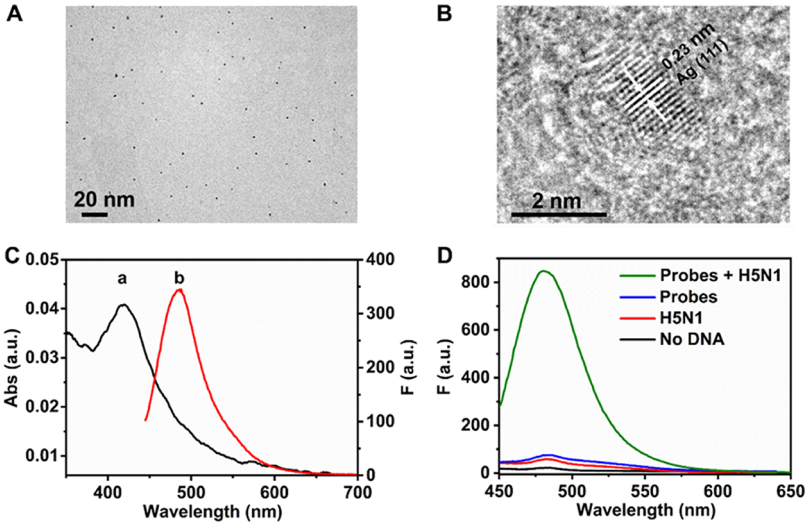

Figure 1. (A) TEM image of DNA-Ag NCs. (B) HRTEM image of a single DNA-Ag NC. (C) UV−vis absorption spectrum (curve a) and corresponding fluorescence emission spectrum (curve b) of DNA-Ag NC aqueous suspension synthesized with probes + H5N1 in CBS. (D) Qualitative detection of H5N1 by the fluorescence changes of the reacted system in the absence and presence of H5N1 (2 μM).

https://dx.doi.org/10.1021/acsami.0c14509
ACS Appl. Mater. Interfaces XXXX, XXX, XXX−XXX

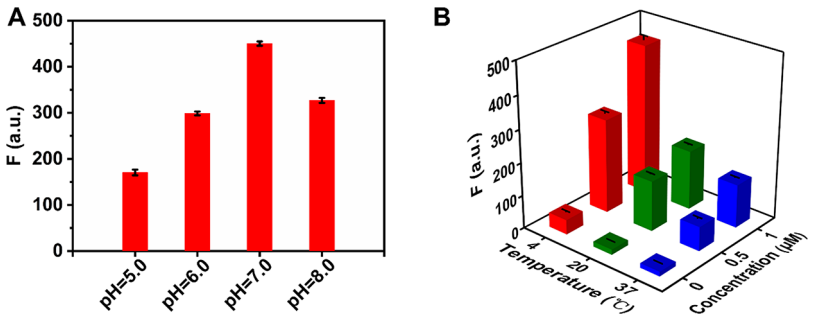

Figure 2. (A) Fluorescence intensity of DNA-Ag NCs prepared under different pH values (5.0, 6.0, 7.0, and 8.0). (B) Fluorescence intensity of DNA-Ag NCs prepared under three different temperatures (4, 20, and 37 °C).

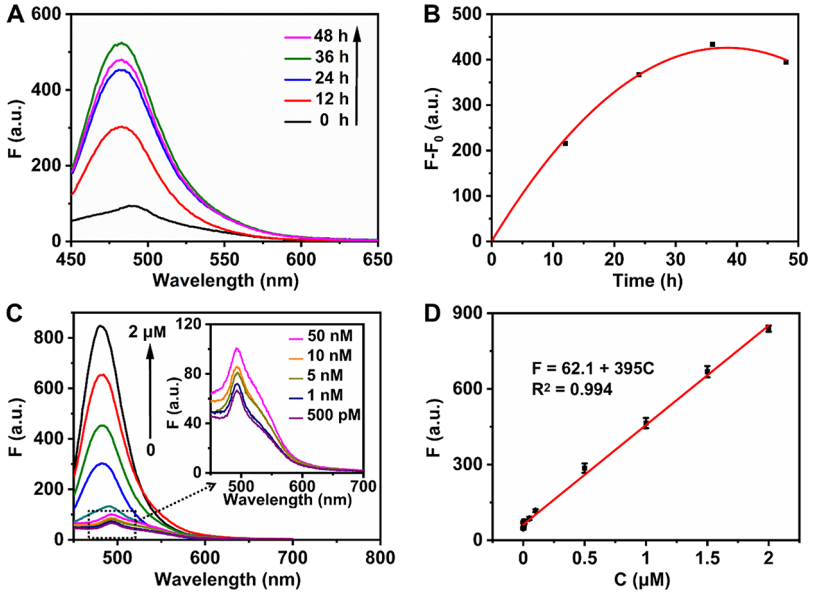

Figure 3. (A) Fluorescence spectra of DNA-Ag NCs at different reaction times with the addition of H5N1 (1 μM). (B) Fluorescence changes of DNA-Ag NCs after adding H5N1 (1 μM) for a different time. F_0 and F represent the fluorescence intensity of the reacted system before and after adding H5N1, respectively. (C) Fluorescence spectra of DNA-Ag NCs in the presence of H5N1 with different concentrations (500 pM, 1 nM, 5 nM, 10 nM, 50 nM, 100 nM, 500 nM, 1 μM, 1.5 μM, 2 μM). (D) Linear curve of F versus the concentration of H5N1 (C).

100 μM) was hybridized with the above probes solution. Other reacted conditions were consistent with the above description for preparing DNA-Ag NCs. All solutions were placed in the dark for 24 h before fluorescence measurements.

Detection of H5N1 in FBS. FBS was diluted 100 times with CBS (pH = 7.0, 20 mM) and then various amounts of H5N1 (100, 500, and 1000 nM) were added into 1% FBS. The amount of each sample was then analyzed by using above fluorescence method based on DNA-Ag NCs.

RESULTS AND DISCUSSION

Synthesis and Characterization of DNA-Ag NCs. Ag^+ bound in the resultant cytosine-rich loop after the probes (P1 and P2) and H5N1 were hybridized and then reduced to Ag NCs by $NaBH_4$. The TEM image (Figure 1A) shows that the formed DNA-Ag NCs have a high degree of dispersion with the average size of less than 2 nm. HRTEM image in Figure 1B displays the interplanar spacing of 0.23 nm attributed to (111) plane of Ag crystals. The UV−vis absorption spectrum (curve a) and fluorescence emission spectrum (curve b) in Figure 1C show that DNA-Ag NCs give a characteristic absorption peak at 420 nm and a corresponding fluorescence emission at 480 nm. The fluorescence emission of DNA-Ag NCs has a typical excitation wavelength-dependent behavior of ultrasmall Ag NCs (Figure S1).

In order to verify the feasibility of analyzing H5N1 through our designed DNA-Ag NC-based strategy, fluorescence emission spectra of the reacted system under different conditions were explored. As shown in Figure 1D, if there is no DNA, or only probes or H5N1 is in the reacted system, its fluorescence is very weak. However, there are approximately 11.10 times of fluorescence enhancement after adding H5N1 to the reacted system containing probes, indicating that only both the probes and H5N1 coexistence can form the fluorescent DNA-Ag NCs in the reacted system. Highly specific base pairing of the H5N1 probes (P1 and P2) and H5N1 allows the formation of a cytosine-rich loop in the buffer solution. Since cytosine has strong affinity for Ag^+, Ag^+ preferentially interacts with cytosine-rich loop in the three-segment-branched DNA structure and is further reduced to Ag NCs by $NaBH_4$. However, Ag NCs cannot be synthesized when H5N1 is not present. Therefore, this sensing method can be applied for qualitative detection of H5N1.

Influence of pH Values and Temperatures on the Formation of DNA-Ag NCs. Fluorescence intensity of DNA-Ag NCs prepared under different pH values (Figure 2A) shows

https://dx.doi.org/10.1021/acsami.0c14509
ACS Appl. Mater. Interfaces XXXX, XXX, XXX−XXX

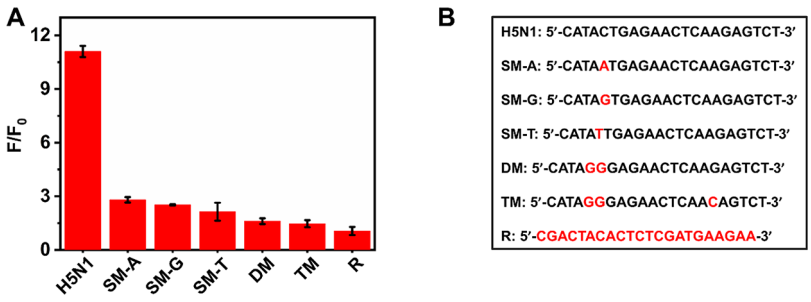

Figure 4. (A) Fluorescence intensity enhancement (F/F_0) of DNA-Ag NCs at 480 nm with the existence of 1 μM H5N1, SM (SM-A, SM-G, and SM-T), DM, TM, and R. SM-A, SM-G, and SM-T are three kinds of DNA with different single-base mismatches, meaning that a single-base C in H5N1 is replaced by A, G, and T, respectively. DM and TM represent two kinds of DNA with double-base and triple-base mismatches, respectively. R: random DNA (H1N1); C: cystosine; A: adenine; G: guanine; T: thymine. (B) Sequences of different types of oligonucleotide used in selective analysis.

Table 1. Ratio of Corresponding Fluorescence Intensity of the Detection System after and before Additions of Different DNA (F/F_0)

parameter	target DNA	single-base mismatched DNA			double-base mismatched DNA	three-base mismatched DNA	random DNA
oligonucleotide	H5N1	SM-A	SM-G	SM-T	DM	TM	R
F/F_0	11.10	2.80	2.52	2.14	1.60	1.47	1.06

that the resultant DNA-Ag NCs at the pH value of 7.0 have the highest fluorescence intensity. Because cytosine tends to be protonized under acidic conditions,[28] cytosine-rich DNA has less force to bind Ag^+ or Ag NCs under acidic conditions, which leads to producing fewer fluorescent DNA-Ag NCs and thus causes the relatively weaker fluorescence of DNA-Ag NCs (pH < 7.0). When the reacted system is basic (pH = 8.0), Ag^+ can react with the phosphate group on the DNA base to form a silver phosphate (Ag_3PO_4) compound, which reduces the amount of Ag^+ interacting with cymidine and also affects the formation of DNA-Ag NCs.[29] Therefore, we chose the pH value of 7.0 for subsequent reactions to detect H5N1. Different concentrations (0, 0.5, and 1 μM) of H5N1 were used to react under different temperatures (4, 20, and 37 °C) to explore the influence of reacted temperature on the fluorescence intensity of DNA-Ag NCs. It can be observed from Figure 2B that the fluorescence of DNA-Ag NCs prepared under the temperature of 4 °C is strongest, indicating that low temperature is beneficial for preparing and stabilizing the formed DNA-Ag NCs.

Kinetic and Quantitative Detection of H5N1. Fluorescence spectra of DNA-Ag NCs with different reaction times were recorded to study the corresponding kinetics of growing DNA-Ag NCs. As shown in Figure 3A,B, the fluorescence of DNA-Ag NCs at 480 nm increases with the reaction time from 0 to 36 h and decreases slightly after 36 h. The reaction time of 24 h is selected to detect H5N1. In order to investigate the sensitivity of our analytical method, different concentrations of H5N1 were added into the buffer solution containing the probes (2 μM) to detect their fluorescence signals. As shown in Figure 3C, the fluorescence intensity of the reacted system increases with the concentration of H5N1, suggesting that the added probes and H5N1 can hybridize to form a cytosine-rich loop to guide the formation of DNA-Ag NCs. The detection limit for H5N1 can reach 500 pM. The fluorescence intensity shows a good linear relationship with the concentration of H5N1 from 500 pM to 2 μM (Figure 3D) (linear relationship from 500 pM−50 nM can be seen in Figure S2) and the linear regression equation is $F = 62.1 + 395C$ ($R^2 = 0.994$). Compared to other previously reported analytical methods, this fluorescence biosensor based on three-segment-branched DNA-Ag NCs has a wider detection range for sensing viral DNA (Table S2). The detection limit of our proposed turn-on fluorescence strategy (500 pM) is lower than the reported single electrode genosensor (20 nM),[30] fluorescence resonance energy transfer (FRET) method (9.39 nM),[31] and fluorescence strategy based on duplex DNA-templated Ag NCs (3.95 nM).[32]

Specific Detection of H5N1. High selectivity is important for the practical applications of biosensors. We used different base-mismatched targets including single-base mismatched DNA (SM), double-base mismatched DNA (DM), triple-base mismatched DNA (TM) and random DNA (R) (the base sequences are listed in Table S1) to replace H5N1 to test the specificity of our fabricated sensing platform. As shown in Figure 4A and Table 1, a fluorescence enhancement of 11.10 times is observed in the presence of H5N1, while there is only an enhancement of 2.80 times for SM and 1.61 times for DM. The fluorescence enhancement for TM and R in the reacted system was also weaker. The experimental results demonstrate that the sensing platform based on fluorescent DNA-Ag NCs is highly specific for H5N1 and can completely distinguish SM (Figure 4B).

Detection of H5N1 in FBS. We further test H5N1 in FBS to explore the practical applications of our analytical method in biological samples. As shown from the detecting results in Table S3, the relative standard deviation (RSD) of this sensing platform based on fluorescent DNA-Ag NCs was less than 7% and the H5N1 recovery was more than 92%, demonstrating the promising applications of our analytical method for sensing H5N1 in the biological and medical fields.

CONCLUSIONS

In summary, a novel fluorescence sensing strategy based on DNA-Ag NCs was designed to detect H5N1, which displays high selectivity, wide linear detection range (500 pM−2 μM), and low LOD (500 pM). Our proposed method for detecting H5N1 displays unique characteristics compared with other reported methods. First, the designed three-segment branched DNA structure to fabricate the fluorescence biosensor based

https://dx.doi.org/10.1021/acsami.0c14509
ACS Appl. Mater. Interfaces XXXX, XXX, XXX−XXX

on DNA-Ag NCs avoids the cumbersome program of labeling with fluorescent dyes and modifying with the recognition molecules. Second, preparing fluorescent DNA-Ag NCs is integrated with targeted recognition of DNA structures and this "on" model is useful for improving sensitivity. Last, our designed DNA template is artful. Three single strands of DNA are hybridized with each other to form a cytosine-rich loop, which breaks through the previous design of cytosine-rich loops formed by hairpin-like single-stranded DNA and double-stranded DNA. This method enriches DNA structures to prepare fluorescent Ag NCs and provides an effective platform for detecting various analytes due to its ease of preparing Ag NCs with the large range of fluorescence emission. It can be powerful to quantify viruses especially for H5N1 in the fields of biological medicine and food analysis.

■ ASSOCIATED CONTENT

Supporting Information

The Supporting Information is available free of charge at https://pubs.acs.org/doi/10.1021/acsami.0c14509.

Sequences of oligonucleotides (from 5′ to 3′ end) used in this work, fluorescence emission spectra of DNA-Ag NCs at different excitation wavelengths, linear relationship between the fluorescence intensity of DNA-Ag NCs and the concentration of H5N1 (500 pM to 50 nM), analytical performance of different methods for detecting viral DNA including H5N1, and detection of H5N1 in fetal bovine serum through the label-free fluorescence method based on DNA-Ag NCs (PDF)

■ AUTHOR INFORMATION

Corresponding Authors

Zhimin Luo − *Key Laboratory for Organic Electronics and Information Displays (KLOEID) & Jiangsu Key Laboratory for Biosensor, Institute of Advanced Materials (IAM), Jiangsu National Synergistic Innovation Center for Advanced Materials (SICAM), College of Electronic and optical Engineering & College of Microelectronic, Nanjing University of Posts and Telecommunications, Nanjing 210023, China*; Email: iamzmluo@njupt.edu.cn

Changfeng Zhu − *Department of Gastroenterology and Hepatology, Zhongshan Hospital, Fudan University, Shanghai 200032, China*; orcid.org/0000-0002-4922-0659; Email: zhuchangfeng@fudan.edu.cn

Lianhui Wang − *Key Laboratory for Organic Electronics and Information Displays (KLOEID) & Jiangsu Key Laboratory for Biosensor, Institute of Advanced Materials (IAM), Jiangsu National Synergistic Innovation Center for Advanced Materials (SICAM), College of Electronic and optical Engineering & College of Microelectronic, Nanjing University of Posts and Telecommunications, Nanjing 210023, China*; Email: iamlhwang@njupt.edu.cn

Authors

Ying Zhang − *Key Laboratory for Organic Electronics and Information Displays (KLOEID) & Jiangsu Key Laboratory for Biosensor, Institute of Advanced Materials (IAM), Jiangsu National Synergistic Innovation Center for Advanced Materials (SICAM), College of Electronic and optical Engineering & College of Microelectronic, Nanjing University of Posts and Telecommunications, Nanjing 210023, China*

Fei Mu − *Key Laboratory for Organic Electronics and Information Displays (KLOEID) & Jiangsu Key Laboratory for Biosensor, Institute of Advanced Materials (IAM), Jiangsu National Synergistic Innovation Center for Advanced Materials (SICAM), College of Electronic and optical Engineering & College of Microelectronic, Nanjing University of Posts and Telecommunications, Nanjing 210023, China*

Yefan Duan − *Key Laboratory for Organic Electronics and Information Displays (KLOEID) & Jiangsu Key Laboratory for Biosensor, Institute of Advanced Materials (IAM), Jiangsu National Synergistic Innovation Center for Advanced Materials (SICAM), College of Electronic and optical Engineering & College of Microelectronic, Nanjing University of Posts and Telecommunications, Nanjing 210023, China*

Qi Li − *Key Laboratory for Organic Electronics and Information Displays (KLOEID) & Jiangsu Key Laboratory for Biosensor, Institute of Advanced Materials (IAM), Jiangsu National Synergistic Innovation Center for Advanced Materials (SICAM), College of Electronic and optical Engineering & College of Microelectronic, Nanjing University of Posts and Telecommunications, Nanjing 210023, China*

Yating Pan − *Key Laboratory for Organic Electronics and Information Displays (KLOEID) & Jiangsu Key Laboratory for Biosensor, Institute of Advanced Materials (IAM), Jiangsu National Synergistic Innovation Center for Advanced Materials (SICAM), College of Electronic and optical Engineering & College of Microelectronic, Nanjing University of Posts and Telecommunications, Nanjing 210023, China*

Hongfang Du − *Key Laboratory for Organic Electronics and Information Displays (KLOEID) & Jiangsu Key Laboratory for Biosensor, Institute of Advanced Materials (IAM), Jiangsu National Synergistic Innovation Center for Advanced Materials (SICAM), College of Electronic and optical Engineering & College of Microelectronic, Nanjing University of Posts and Telecommunications, Nanjing 210023, China*

Panpan He − *Key Laboratory for Organic Electronics and Information Displays (KLOEID) & Jiangsu Key Laboratory for Biosensor, Institute of Advanced Materials (IAM), Jiangsu National Synergistic Innovation Center for Advanced Materials (SICAM), College of Electronic and optical Engineering & College of Microelectronic, Nanjing University of Posts and Telecommunications, Nanjing 210023, China*

Xizhong Shen − *Department of Gastroenterology and Hepatology, Zhongshan Hospital, Fudan University, Shanghai 200032, China*

Complete contact information is available at: https://pubs.acs.org/10.1021/acsami.0c14509

Author Contributions

Designing and writing: Z.Y. Investigation: F.M. and Y.D. Characterization: Q.L., Y.P., and H.D. Analysis: P.H. Methodology: X.S. Conceptualization and supervision: Z.L., C.Z. and L.W.

Notes

The authors declare no competing financial interest.

■ ACKNOWLEDGMENTS

This work was financially supported by the National Key Research and Development Program of China (2017YFA0205302), the National Natural Science Foundation of China (21475064, 61705113), the Program for Changjiang Scholars and Innovative Research Team in University

(IRT_15R37), the Key Research and Development Program of Jiangsu (BE2018732), the Natural Science Key Fund for Colleges and Universities in Jiangsu Province (17KJA430011), the National Postdoctoral Program for Innovative Talents (BX20190156), Key Grant for Special Professors in Jiangsu Province (RK030STP18001), the China Scholarship Council (CSC201808320013), the Scientific Research Foundation of Nanjing University of Posts and Telecommunications (NY217007, NY218150), and Training Program of the Major Research Plan of the National Natural Science Foundation of China from Nanjing University of Posts and Telecommunications (NY218158).

REFERENCES

(1) Li, Y.; Wang, R. Aptasensors for Detection of Avian Influenza Virus H5N1. *Methods Mol. Biol.* **2017**, *1572*, 379−402.
(2) Shinya, K.; Ebina, M.; Yamada, S.; Ono, M.; Kasai, N.; Kawaoka, Y. Avian Flu: Influenza Virus Receptors in the Human Airway. *Nature* **2006**, *440*, 435−436.
(3) Berns, K. I.; Casadevall, A.; Cohen, M. L.; Ehrlich, S. A.; Enquist, L. W.; Fitch, J. P.; Franz, D. R.; Fraser-Liggett, C. M.; Grant, C. M.; Imperiale, M. J.; Kanabrocki, J.; Keim, P. S.; Lemon, S. M.; Levy, S. B.; Lumpkin, J. R.; Miller, J. F.; Murch, R.; Nance, M. E.; Osterholm, M. T.; Relman, D. A.; Roth, J. A.; Vidaver, A. K. Adaptations of Avian Flu Virus Are a Cause for Concern. *Science* **2012**, *335*, 660−661.
(4) Comin, A.; Toft, N.; Stegeman, A.; Klinkenberg, D.; Marangon, S. Serological Diagnosis of Avian Influenza in Poultry: Is the Haemagglutination Inhibition Test Really the 'Gold Standard'? *Influenza Other Respir. Viruses* **2013**, *7*, 257−264.
(5) Horm, S. V.; Tarantola, A.; Rith, S.; Ly, S.; Gambaretti, J.; Duong, V.; Y, P.; Sorn, S.; Holl, D.; Allal, L.; Kalpravidh, W.; Dussart, P.; Horwood, P. F.; Buchy, P. Intense Circulation of A/H5N1 and Other Avian Influenza Viruses in Cambodian Live-Bird Markets with Serological Evidence of Sub-Clinical Human Infections. *Emerging Microbes Infect.* **2016**, *5*, No. e70.
(6) Bai, H.; Wang, R.; Hargis, B.; Lu, H.; Li, Y. A SPR Aptasensor for Detection of Avian Influenza Virus H5N1. *Sensors* **2012**, *12*, 12506−12518.
(7) Lin, J.; Wang, R.; Jiao, P.; Li, Y.; Li, Y.; Liao, M.; Yu, Y.; Wang, M. An Impedance Immunosensor Based on Low-Cost Microelectrodes and Specific Monoclonal Antibodies for Rapid Detection of Avian Influenza Virus H5N1 in Chicken Swabs. *Biosens. Bioelectron.* **2015**, *67*, 546−552.
(8) Kim, Y. T.; Jung, J. H.; Choi, Y. K.; Seo, T. S. A Packaged Paper Fluidic-Based Microdevice for Detecting Gene Expression of Influenza A Virus. *Biosens. Bioelectron.* **2014**, *61*, 485−490.
(9) Shisong, F.; Jianxiong, L.; Xiaowen, C.; Cunyou, Z.; Ting, W.; Xing, L.; Xin, W.; Chunli, W.; Renli, Z.; Jinquan, C.; Hong, X.; Muhua, Y. Simultaneous Detection of Influenza Virus Type B and Influenza A Virus Subtypes H1N1, H3N2, and H5N1 Using Multiplex Real-Time RT-PCR. *Appl. Microbiol. Biotechnol.* **2011**, *90*, 1463−1470.
(10) Feng, D.-Q.; Liu, G.; Wang, W. A Novel Biosensor for Copper(ii) Ions Based on Turn-On Resonance Light Scattering of SsDNA Templated Silver Nanoclusters. *J. Mater. Chem. B* **2015**, *3*, 2083−2088.
(11) Guo, W.; Yuan, J.; Dong, Q.; Wang, E. Highly Sequence-Dependent Formation of Fluorescent Silver Nanoclusters in Hybridized DNA Duplexes for Single Nucleotide Mutation Identification. *J. Am. Chem. Soc.* **2010**, *132*, 932−934.
(12) Richards, C. I.; Choi, S.; Hsiang, J. C.; Antoku, Y.; Vosch, T.; Bongiorno, A.; Tzeng, Y. L.; Dickson, R. M. Oligonucleotide-Stabilized Ag Nanocluster Fluorophores. *J. Am. Chem. Soc.* **2008**, *130*, 5038−5039.
(13) Teng, Y.; Tateishi-Karimata, H.; Tsuruoka, T.; Sugimoto, N. A Turn-On Detection of DNA Sequences by Means of Fluorescence of DNA-Templated Silver Nanoclusters via Unique Interactions of a Hydrated Ionic Liquid. *Molecules* **2018**, *23*, 2889.
(14) Han, Y.; Zhang, F.; Gong, H.; Cai, C. Multifunctional G-quadruplex-Based Fluorescence Probe Coupled with DNA-Templated AgNCs for Simultaneous Detection of Multiple DNAs and MicroRNAs. *Anal. Chim. Acta* **2019**, *1053*, 105−113.
(15) Feng, X.; Han, T.; Xiong, Y.; Wang, S.; Dai, T.; Chen, J.; Zhang, X.; Wang, G. Plasmon-Enhanced Electrochemiluminescence of Silver Nanoclusters for Microrna Detection. *ACS Sens.* **2019**, *4*, 1633−1640.
(16) Liu, G.; Li, J.; Feng, D.-Q.; Zhu, J.-J.; Wang, W. Silver Nanoclusters Beacon as Stimuli-Responsive Versatile Platform for Multiplex DNAs Detection and Aptamer-Substrate Complexes Sensing. *Anal. Chem.* **2017**, *89*, 1002−1008.
(17) Li, B.; Chen, Y.; Wang, J.; Lu, Q.; Zhu, W.; Xu, L.; Shen, X.; Luo, J.; Zhu, C.; Li, X.; Hong, J.; Zhou, X. DNA-Silver Nanoclusters/Polypyrrole Nanoparticles: A Label-Free and Enzyme-Free Platform for Multiplexed Transcription Factors Detection. *Sens. Actuators, B* **2018**, *274*, 481−490.
(18) Zhang, Y.; Zhu, C.; Zhang, L.; Tan, C.; Yang, J.; Chen, B.; Wang, L.; Zhang, H. DNA-Templated Silver Nanoclusters for Multiplexed Fluorescent DNA Detection. *Small* **2015**, *11*, 1385−1389.
(19) Zou, R.; Zhang, F.; Chen, C.; Cai, C. DNA-Programming Multicolor Silver Nanoclusters for Sensitively Simultaneous Detection of Two HIV DNAs. *Sens. Actuators, B* **2019**, *296*, 126608.
(20) Xu, J.; Wei, C. The Aptamer DNA-Templated Fluorescence Silver Nanoclusters: ATP Detection and Preliminary Mechanism Investigation. *Biosens. Bioelectron.* **2017**, *87*, 422−427.
(21) Park, K. S.; Oh, S. S.; Soh, H. T.; Park, H. G. Target-Controlled Formation of Silver Nanoclusters in Abasic Site-Incorporated Duplex DNA for Label-Free Fluorescence Detection of Theophylline. *Nanoscale* **2014**, *6*, 9977−9982.
(22) Liu, G.; Feng, D. Q.; Mu, X.; Zheng, W.; Chen, T.; Qi, L.; Li, D. DNA-Functionalized Silver Nanoclusters as a Chemopalette: Tunable Fluorescence for Turn-On Detection of Cysteine. *J. Mater. Chem. B* **2013**, *1*, 2128−2131.
(23) Park, J.; Song, J.; Park, J.; Park, N.; Kim, S. Branched DNA-Based Synthesis of Fluorescent Silver Nanocluster. *Bull. Korean Chem. Soc.* **2014**, *35*, 1105−1109.
(24) Yang, L.; Yao, C.; Li, F.; Dong, Y.; Zhang, Z.; Yang, D. Synthesis of Branched DNA Scaffolded Super-Nanoclusters with Enhanced Antibacterial Performance. *Small* **2018**, *14*, No. e1800185.
(25) Gwinn, E. G.; O'Neill, P.; Guerrero, A. J.; Bouwmeester, D.; Fygenson, D. K. Sequence-Dependent Fluorescence of DNA-Hosted Silver Nanoclusters. *Adv. Mater.* **2008**, *20*, 279−283.
(26) Xia, X.; Hao, Y.; Hu, S.; Wang, J. Hairpin DNA Probe with 5'-TCC/CCC-3' Overhangs for the Creation of Silver Nanoclusters and MiRNA Assay. *Biosens. Bioelectron.* **2014**, *51*, 36−39.
(27) Petty, J. T.; Zheng, J.; Hud, N. V.; Dickson, R. M. DNA-Templated Ag Nanocluster Formation. *J. Am. Chem. Soc.* **2004**, *126*, 5207−5212.
(28) Liu, B.; Liu, J. Accelerating Peroxidase Mimicking Nanozymes Using DNA. *Nanoscale* **2015**, *7*, 13831−13835.
(29) Lee, J. D.; Cang, J.; Chen, Y.-C.; Chen, W.-Y.; Ou, C.-M.; Chang, H.-T. Detection of Adenosine 5′-Triphosphate by Fluorescence Variation of Oligonucleotide-Templated Silver Nanoclusters. *Biosens. Bioelectron.* **2014**, *58*, 266−271.
(30) Grabowska, I.; Malecka, K.; Stachyra, A.; Góra-Sochacka, A.; Sirko, A.; Zagórski-Ostoja, W.; Radecka, H.; Radecki, J. Single Electrode Genosensor for Simultaneous Determination of Sequences Encoding Hemagglutinin and Neuraminidase of Avian Influenza Virus Type H5N1. *Anal. Chem.* **2013**, *85*, 10167−10173.
(31) Tian, J.; Zhao, H.; Liu, M.; Chen, Y.; Quan, X. Detection of Influenza A Virus Based on Fluorescence Resonance Energy Transfer From Quantum Dots to Carbon Nanotubes. *Anal. Chim. Acta* **2012**, *723*, 83−87.
(32) Han, D.; Wei, C. A Molecular Beacon Based on DNA-Templated Silver Nanoclusters for the Highly Sensitive and Selective Multiplexed Detection of Virulence Genes. *Talanta* **2018**, *181*, 24−31.

https://dx.doi.org/10.1021/acsami.0c14509
ACS Appl. Mater. Interfaces XXXX, XXX, XXX−XXX